Jordan Journal of Civil Engineering, Volume **20**, No. **4**, **2026**
DOI: https://doi.org/10.14525/JJCE.v20i4.02

Jordan Journal of Civil Engineering

Journal homepage: https://jjce.just.edu.jo

Deflection Behavior of Concrete Pipe Jacking in Rock Strata: Field Tests and Damage Modeling

Jiawei Wang [1], Kaifeng Cao [1], Xin Feng [1] *, Keqin Zhang [1], Kang Dong [1], Yinliang Zhou [1]

[1] *Changjiang International Hydro Engineering Company Ltd, Wuhan 430040, China.*
** Corresponding Author. E-Mail: gcxy321@163.com*

ARTICLE INFO

Article History:
Received: 31/7/2025
Accepted: 28/3/2026

ABSTRACT

This study addresses the unclear damage mechanisms of the pipe during long-distance pipe jacking in highly permeable rock strata. This paper combines field monitoring and numerical simulation of a pipe jacking project to reveal the causes of pipe cracking and the relationship between damage patterns and deflection angles. Analysis of the full-cycle measured data on rebar stress, concrete strain, contact pressure, and mud pressure reveals that the fundamental cause of pipe segment cracking is stress redistribution induced by pipe deflection. It is further shown that the severe fluctuations in the monitoring data are due to a cyclic process of "deflection → correction → re-deflection". Through numerical simulations, the non-linear relationship between deflection angle and the ultimate jacking force is quantified. The results show a strong correlation between the damage patterns of the pipe segments and the deflection angle. Specifically, small-angle deflections are characterized by diagonal cracks in the pipe barrel, while large-angle deflections lead to radial crushing damage at the joints. These results offer important guidance for improving construction parameters and developing effective damage control strategies in upcoming pipe jacking projects within rock strata.

Keywords: Rock strata, Deflection behavior, Cracks, Field testing, Numerical simulation.

INTRODUCTION

As a trenchless construction technique, pipe jacking offers high efficiency, enhanced safety, and minimal environmental impact, making it essential for advancing urban subterranean infrastructure development (Ma, 2008; Ma & Najafi, 2008; Bergeson, 2014). However, the mechanical interaction and stress transfer behavior at the pipe-soil interface during pipe jacking construction remain critical determinants of project safety. This is particularly prominent under complex working conditions, where deflection of the pipe segments — a frequent occurrence during construction — can cause stress redistribution, resulting in cracking and posing a significant threat to construction safety. Therefore, conducting a thorough study of the mechanical properties of pipe segments in rock strata, along with understanding the concrete damage progression caused by pipe segment deflection, is essential for ensuring construction safety and facilitating the successful progress of the project.

In investigating the stress behavior of pipe segments, Milligan and Norris (1996; 1999) deployed monitoring instruments at the pipe jacking construction site to measure the angular deviation, stress distribution, longitudinal strain, axial strain, shear stress, and contact pressure at the pipe segment joints. Zhang et al. (2022; 2023), in their research on the curved pipe jacking project, installed monitoring instruments on the pipe segments to monitor axial and hoop strains as well as contact pressure, investigating the distribution and variation of axial hoop strains, and contact pressure under deep burial conditions during construction. Through *in-situ* monitoring of reinforced concrete pipe jacking operations, Wei et al. (2005) quantified the temporal evolution of pipe-soil contact stresses and segmental strain response patterns. Liu et al. (2022) focused on the issue of pipe sticking in rock strata, investigating the frictional characteristics at the steel pipe-rock interface and their impact. Zhang et al. (2022), based on the Suzhou rectangular shield tunneling project, monitored the contact pressure throughout the entire construction cycle. The study revealed the dynamic evolution of earth pressure around the pipe under grout lubrication. Zhou et al. (2023) focused on the use of PSO-BPNN and PSO-SVR algorithms to predict the jacking force of curved pipes, highlighting the significance of advanced prediction methods in tunnel engineering. Through full-scale experimental tests and numerical modeling, Liu et al. (2024) quantified how pipe joint deflection influences axial stress patterns and jacking force transmission mechanisms. He et al. (2024) elucidated how joint deflection governs the axial stress-strain response of reinforced concrete pipelines during curved pipe jacking operations. Li (2020) developed a 3D model of pipe joint deflection using ABAQUS finite element software, revealing the functional dependence of joint structural limit states on angular deviation magnitude. Tong et al. (2020) analyzed the stress state of pipe segments under same-side and diagonal offset pressure conditions, developed a refined calculation model for the offset pressure state of pipe segments, and proposed control measures for pipe jacking offset pressure. Xu et al. (2025) employed a combined approach of laboratory testing and numerical simulation to conduct systematic research on the mechanical properties of rectangular pipe jacking joints equipped with longitudinal connectors. The study clarified the process and critical regions of shear failure in the joints, confirming the effective role of longitudinal connectors in controlling damage to rectangular pipe jacking joints. Hasani (2025) utilized ABAQUS numerical simulation software to establish a series of joint models for concrete-filled steel tubes (CFSTs). The study investigated the influence of multiple parameters on the load-bearing capacity and stress-strain behavior of K-type joints.

Despite considerable results of research on the stress characteristics of pipe segments, the mechanical behavior of pipe segments in rock formations and the concrete damage evolution induced by pipe segment deflection remain unclear. Therefore, this paper focuses on the Danjiangkou river-crossing pipe jacking project in rock strata, conducting comprehensive field monitoring of contact pressure, mud pressure, and axial stress and strain in the pipe segments throughout the entire jacking process. A thorough analysis of the stress condition of the pipe segments is conducted, and, in conjunction with the pipe deflection conditions, a 3D model of pipe deflection is established using ABAQUS finite element software. This study investigates the evolution of concrete damage under different deflection conditions in greater detail.

Project Profile

This study is based on the Danjiangkou Urban Water Supply Capacity Enhancement Project, which involves the installation of approximately 10 km of water transmission pipelines. The focus of this research is on the pipe jacking project in the segment crossing the Han River, specifically the straight-line pipe jacking section. The overall jacking length for the project measures 718 meters, with a single-stage continuous jacking. Fig.1 shows the physical parameters of each layer. The thickness of the overburden from the pipe segment to the riverbed ranges from 6.2 to 14.5 meters, mainly passing through moderately weathered metamorphic diabase, strongly weathered metamorphic diabase, moderately weathered conglomerate, and moderately weathered muddy siltstone. The physical parameters of each stratum are provided in Table 1. Among them, the strongly weathered metamorphic diabase has well-developed fractures, with a fractured rock mass and a permeability ranging from 19 to 46 Lu, indicating moderate permeability. The moderately weathered diabase has a permeability ranging from 6.48 to 10.66 Lu, indicating weak permeability.

The pipe jacking process employs C50 pre-cast reinforced concrete pipe segments, each with an outer diameter of 2.4 meters, an inner diameter of 2.0 meters, and a length of 2.5 meters per segment. The pipes are classified as having a water resistance grade of P8. The joints are of the F-type spigot and socket design, with two wedge-shaped rubber seals installed, as shown in Fig. 2.

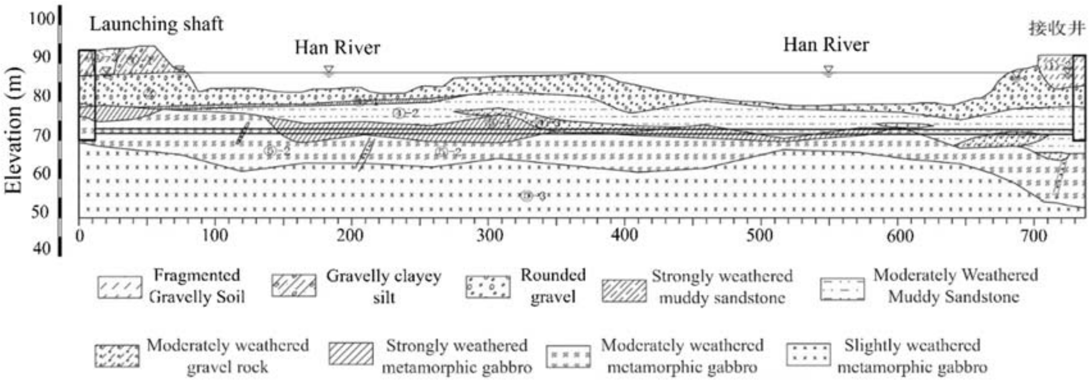

Figure 1. Profile diagram of the strata crossed by the pipe jacking

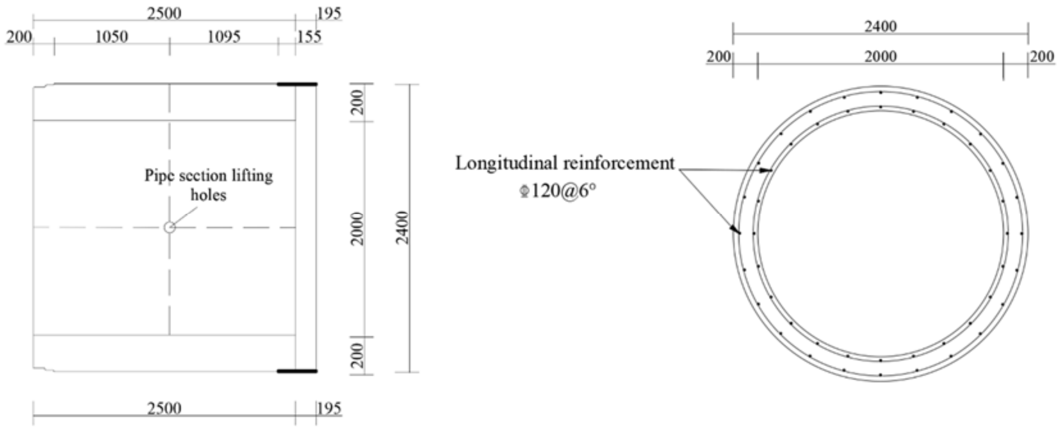

Figure 2. Pipe segment structure

Table 1. Physical and mechanical parameters of the strata

Strata Types	**Natural unit weight γ (kN/m^3)**	**Cohesion c (kPa)**	**Internal friction angle φ (°)**	**Foundation bearing capacity characteristic value f_{ak} (kPa)**	**Permeability (Lu)**	**Compressive strength f_r(MPa)**
Moderately weathered metamorphic gabbro and diabase	28.9	1000	43.5	3200	6.5~10.7	17.43
Highly weathered metamorphic gabbro and diabase	27.1	450	28.8	1200	19~46	10.85
Moderately weathered conglomerate	25.9	550	31	1100	/	10.5
Moderately weathered mudstone and silty sandstone	23.8	330	24.2	800	1.34	7.45

Field Monitoring Plan

Throughout the river-crossing section of the pipe jacking process, the pipe often passes through various rock strata. In order to ensure the structural stability of the pipeline throughout the pipe jacking process, field tests were performed using strain gauges, concrete strain gauges, soil pressure sensors, and slurry pressure meters to track the stress parameters of the pipe segments. These monitored parameters include the circumferential contact pressure, external water pressure, axial stress in the steel reinforcement, and axial strain in the concrete.

The monitoring section of the project is located at pipe segments #241 and #251. The configuration of the monitoring section is illustrated in Fig.3. Earth pressure gauges (numbered E-1 to E-4) and mud pressure gauges (numbered P-1 to P-4) are arranged every 90° along the circumference of the monitoring section. Additionally, axial strain gauges for reinforcement (numbered S-1 to S-8) and axial strain gauges for concrete (numbered C-1 to C-8) are placed at every 45°. The axial strain gauges for the reinforcement are welded onto the external reinforcement cage of the pipe segment, whereas the axial concrete strain gauges are fixed to the outer reinforcement cage with high-strength cable ties. The front end of the concrete block of the axial concrete strain gauges is made of C50 concrete, which is consistent with the concrete used for casting the pipe segment. The on-site layout is shown in Fig. 4.

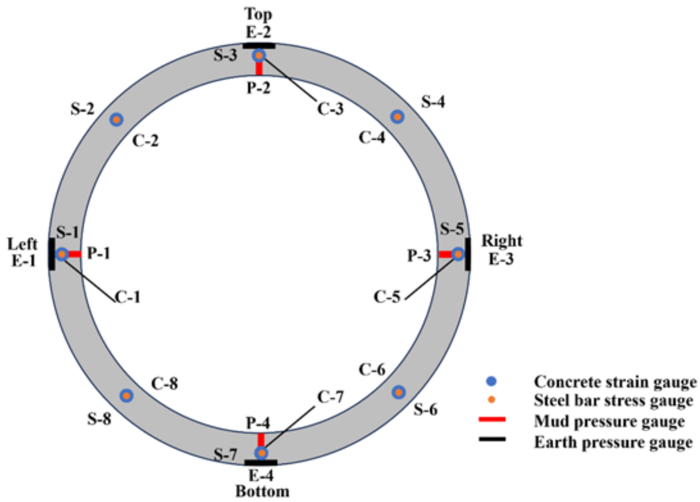

Figure 3. Monitoring section layout plan

(a) Stress gauge and strain gauge installation

(b) Mud pressure gauge and earth pressure gauge installation

Figure 4. On-site sensor layout diagram

The data output signals from the earth pressure gauges, mud pressure gauges, stress gauges and strain gauges used in the experiment are string vibration signals. These signals are collected by the MCU acquisition unit, which is then connected to the LoRa and 4G DTU communication devices. The data is uploaded in real time to the cloud platform. Through the real-time calculation functionality of the cloud platform, the acquired data is transformed into intuitive parameters, such as pipe segment stress and strain, contact pressure, and mud pressure. During construction, to ensure the timeliness of the data, the collection frequency for each monitoring point is set to once every 10 minutes. The monitoring principle is illustrated in Fig.5. The on-site construction and monitoring cross-section layouts are shown in Fig. 6.

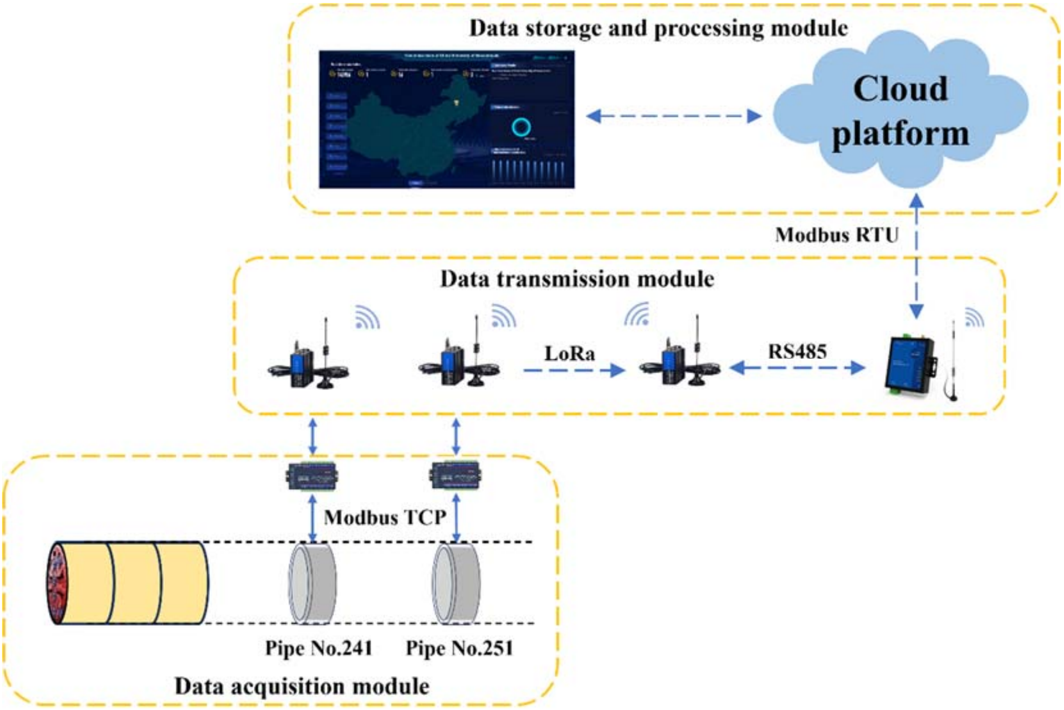

Figure 5. Monitoring principle

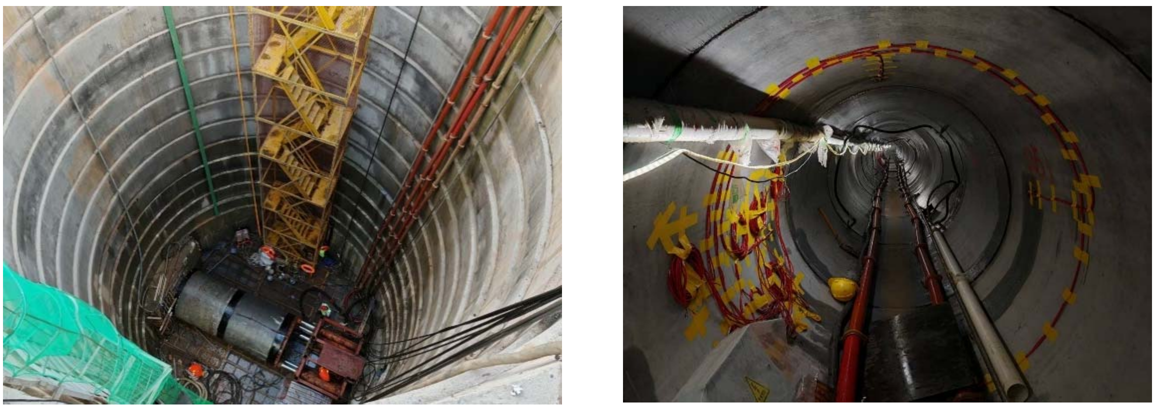

(a) On-site construction (b) Monitoring cross-section

Figure 6. On-site construction and monitoring cross-section

ANALYSIS OF MONITORING RESULTS

On July 11-12, 2024, during the pipe jacking process, surface micro-cracks unexpectedly appeared on the bottom-left side of the Pipe #251 at a location between 50 and 52.5 meters from the tunnel entrance. The location and shape of the cracks are shown in Fig.7 and Fig. 8, respectively. To further investigate the causes of crack formation during passage through this section, a detailed analysis was conducted on the axial stress, axial strain, contact pressure around the pipe segment, and mud pressure for the Pipe #251 when passing through this interval. This analysis aims to identify the potential factors contributing to the crack formation and to propose corresponding measures to ensure that similar issues do not occur in subsequent construction.

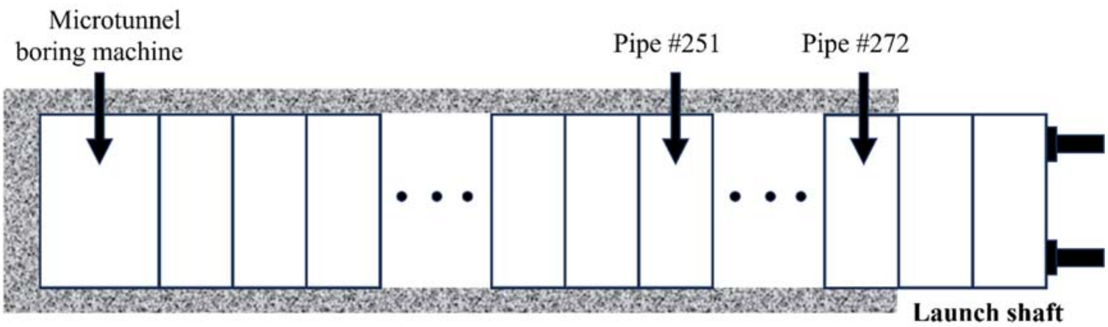

Figure 7. The location of the crack

Figure 8. The shape of the crack

For ease of comparative analysis, the on-site monitoring data of the Pipe #251 from July 10 to 13, 2024, was extracted, and the mechanical data of the pipe segment was divided into three regions. Regions ① and ③ represent the normal jacking phase, while region ② corresponds to the phase when the cracks appeared. Fig.9 and Fig.10 display the variation trends of contact pressure around the pipe segment and mud pressure around the pipe segment during its passage through the weathered and metamorphic gabbro layer from July 10 to 14, 2024. The monitoring results indicate that, during the normal jacking phase, the contact pressures on both sides of the pipe segment and the mud pressures are approximately equal, with an average difference of less than 10 kPa. Furthermore, the trends in the contact pressure and mud pressure around the pipe are almost identical. Mud pressure at the top of the pipe segment is the highest, considerably surpassing that at the bottom, while the contact pressure at the bottom is the greatest and significantly exceeds that at the top. These observations suggest that during the jacking process, the pipe segment did not experience uplift; instead, its bottom remained in close contact with the surrounding rock, maintaining a higher contact pressure. Furthermore, as grouting in this project was primarily performed at the top of the pipe segment, the grout had difficulty effectively permeating to the mud pressure gauge at the bottom, which resulted in the mud pressure at the bottom remaining relatively low. The general fluctuation trends of the contact pressure and mud pressure around the pipe segment indicate that the contact pressure is mainly influenced by the mud pressure.

As shown in Fig.9, it is evident that once Pipe #251 transitions into phase ②, the contact pressure on its right side rises sharply, reaching a peak value of 450 kPa, even exceeding the contact pressure at the bottom of the pipe segment. As pipe segment progresses, the contact pressure on the right rear side shows significant fluctuations, characterized by a sharp rise followed by a sudden drop. After a brief period of stabilization, the pressure fluctuates sharply again, while the mud pressure shows no similar changes. A preliminary assumption is that the notable fluctuations in the contact pressure on the right side of the pipe segment could suggest the development of a crack. To verify this hypothesis and investigate the underlying cause of this abnormal phenomenon, a thorough analysis should be performed by integrating the monitoring data of the steel reinforcement stress and concrete strain for Pipe #251.

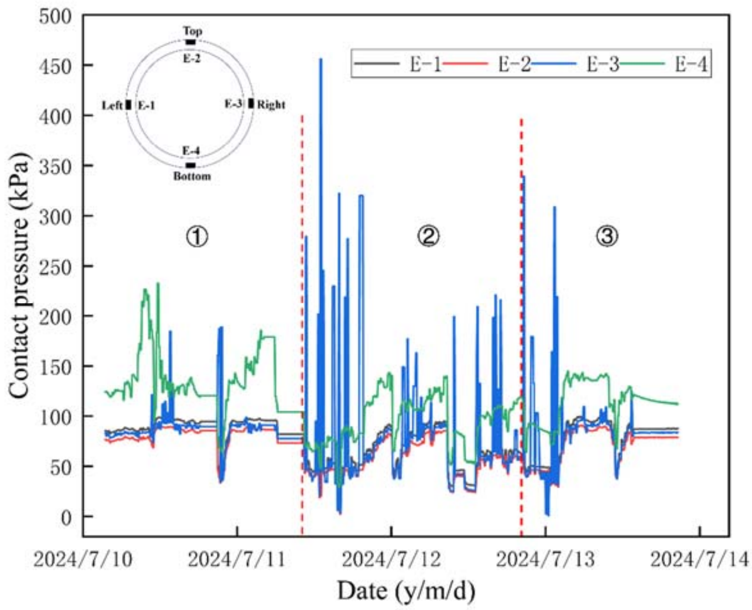

Figure 9. Contact pressure of pipe segment # 251from July 10th to 14th

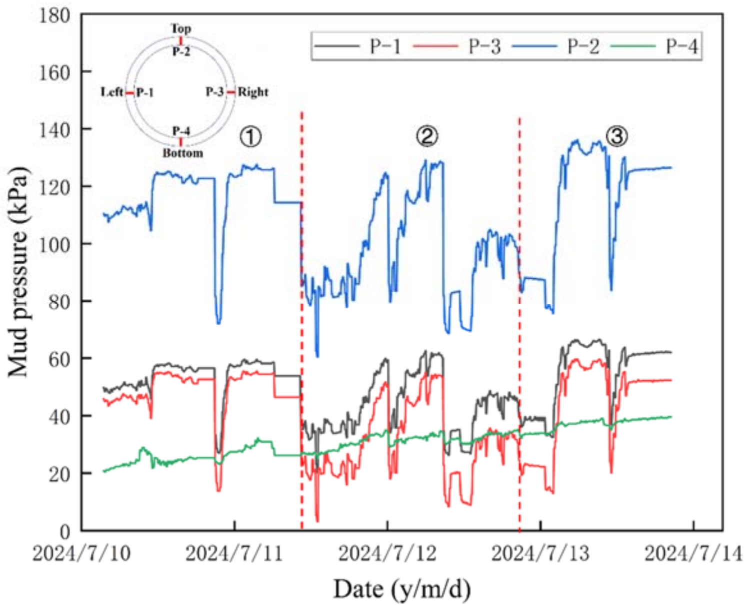

Figure 10. Mud pressure of pipe segment #251 from July 10th to 14th

The monitoring data of the steel reinforcement stress for the Pipe #251 are shown in Fig. 11. (supplementary data) As seen in Fig.11 (supplementary data), under normal jacking conditions, except for occasional small tensile stresses at the bottom-left side of the pipe segment, the axial stress of the pipe segment is primarily compressive. Overall, the steel strain gauges at each monitoring point exhibit consistent trends in stress variation, and there is no significant difference in axial steel reinforcement stress values at different spatial locations of the pipe segment. However, once the pipe segment enters phase ②, the steel reinforcement stress values at various locations of the pipe segment undergo noticeable changes. Specifically, the compressive stresses on the upper right side (S-4) and right side (S-5) slightly decrease, while the compressive stress on the left side (S-1) slightly increases. A significant rise in compressive stress is also observed at the bottom of the pipe segment (S-7). The most pronounced change occurs at the bottom-left side of the pipe segment (S-8), where the compressive stress suddenly increases from 1 kN to 10 kN. Subsequently, during this jacking interval, the compressive stress fluctuates significantly, with the average stress maintaining around 7.8 kN. Notably, the axial stress values at the bottom-left side (S-8) and the bottom (S-7) of the pipe segment remain the highest throughout this interval.

Fig. 12 (supplementary data) presents the monitoring data of the axial strain in the concrete at the bottom-left side (S-8) of the Pipe #251. As illustrated in Fig.12, the axial strain in the concrete closely follows the changes in the axial stress of the steel reinforcement. When the pipe segment enters phase ②, the strain monitoring reveals critical compressive strain accumulation in the lower-left pipe region, with values surging from approximately -300 με to about -600 με, displaying significant fluctuations throughout this jacking interval. The fluctuation pattern is similar to that of the compressive steel stress at the bottom-left side (S-8), with some peaks even reaching -1200 με. The control values for tensile and compressive strain in C50 concrete are 100 με and -1712 με, respectively (Zhang et al., 2017). Although the maximum compressive strain in the concrete does not exceed the design limit of -1712 με, thus posing no risk of structural failure, there remains a potential risk of inducing microcracks on the surface of the pipe segment.

Based on the asymmetric stress/strain distribution characteristics revealed by the monitoring data, combined with the phenomenon of significant and abnormal fluctuations in the contact pressure on the right side of the pipe segment, as well as key information from the construction logs indicating frequent alignment corrections of the microtunnel boring machine without a corresponding reduction in jacking force during this period, a thorough analysis indicates that the surface microcracks on the bottom-left side of the pipe segment are mainly due to the segment's deflection relative to the design axis. This deflection causes the segment to shift upward and to the right throughout the pipe jacking procedure, with inadequate adjustment of the jacking force. This deflection leads to a redistribution of the axial compressive stress within the pipe segment, forming a significant stress concentration zone on its lower-left side, which directly explains the sharp increase in both the axial steel reinforcement stress and the concrete compressive strain monitored in this region (S-8). Simultaneously, as the deflection of the pipe segment increases, its contact with the surrounding rock and soil on the right side also increases, leading to an abnormal rise in the contact pressure on that side. After the alignment correction by the microtunnel boring machine, the stress state of the pipe segment temporarily returns to normal. However, as the pipe segment experiences deflection again, the operators perform another round of alignment corrections. This repetitive cycle is the fundamental cause of the significant fluctuations observed in the monitoring data of the pipe.

To prevent the recurrence of similar issues in subsequent construction, a sensing parameter early warning system has been introduced in the cloud platform for this project. The operational mechanism of the system is as follows:

(1) Inclinometers are installed between the spigot and bell ends of subsequently jacked pipe segments. After each segment is jacked, the monitoring system collects and uploads real-time data on the mechanical behavior of the test pipe segments and the deflection angles between newly jacked pipe segments.

(2) The warning system continuously monitors and analyzes the uploaded mechanical and deflection data against predefined thresholds. The threshold for pipe segment deflection angle is set at 0.5°, as detailed in the following section.

If any segment's data exceeds the threshold values, the system automatically triggers a warning and notifies the staff. This enables timely identification of potential risks and allows for targeted corrective actions, such as adjusting the direction of the microtunnel boring machine or increasing the injection volume of lubricating slurry.

Additionally, by properly controlling the jacking force and adding intermediate jacking stations, sufficient jacking force is reserved for the jacking interval, thus preventing excessive pressure from being applied by the main hydraulic jacks due to insufficient forward jacking force, which could otherwise lead to structural damage of the pipe segments. In subsequent construction phases, although some segments still experienced deflection angles exceeding 0.5°, the timely warnings issued by the system allowed the construction team to take appropriate measures. Consequently, the monitored stress data of the segments remained within normal fluctuation ranges. No further cracking of the pipe segments occurred, effectively eliminating such quality hazards.

Numerical Simulation of Concrete Damage Development

Model Development and Material Parameters

During pipe jacking construction, factors, such as variations in geological conditions, equipment precision limitations, and interactions between pipe segments, can cause deviations from a straight jacking trajectory, leading to deflection between the segments. If the jacking force is applied improperly under such conditions, cracks or even failure of the pipe segments may occur. To determine the ultimate jacking force under deflection conditions and systematically analyze the effect of continuously increasing jacking force on concrete damage development, this study created a numerical model for pipe segment deflection using Abaqus software, as illustrated in Fig. 13 (supplementary data) and Fig. 14 (supplementary data). In this model, the geometric dimensions of the pipe segment, steel casing, and wooden spacers are strictly defined based on the actual components from the field, as illustrated in Fig. 2.

Basic Assumptions

For the overall pipe segment model, each pipe segment is designed with a spigot end and a bell end. At the joint bell of each pipe segment, a tie constraint is applied between the bell and the wooden spacer, as well as between the bell and the steel casing, to eliminate relative sliding between materials. At the spigot end joint, a contact relationship is established between the spigot and the wooden spacer, as well as between the spigot and the steel casing. To more accurately simulate the actual working conditions, the following assumptions are made for the model:

(1) The model utilizes the Concrete Damage Plasticity approach, incorporated within the Abaqus platform, to simulate the concrete's mechanical behavior, while the steel casing and spacers are treated as ideal elastic-plastic materials. The material properties, including the elastic modulus and Poisson’s ratio, remain constant throughout the simulation.

(2) This study focuses on the structural failure of concrete at pipe joints under angular deflection. In practice, for non-pressure pipelines, the compression ratios of both the wedge-shaped rubber seal at the spigot end and the water-swelling rubber seal at the bell end are very small. During pipe deflection, these rubber seals exert only minor radial contact pressures on the spigot, which are negligible compared to the axial compressive stresses and have little effect on the overall stress distribution in the pipe. Moreover, these rubber seals primarily govern joint watertightness rather than mechanical performance (Zhou et al., 2025). Therefore, the influence of the rubber seals at the pipe joints is not considered in the model, and the rubber seals are not explicitly modeled.

(3) This model primarily investigates the mechanical behavior of the concrete at the pipe joint. Therefore, detailed modeling is conducted for the concrete lining at the pipe joint, the steel casing, and the bell and spigot interface to improve the computational accuracy.

Material Parameters

In the numerical model, the concrete is assigned an elastic modulus of 34.5 GPa, a density of 2,400 kg/m³, and a Poisson’s ratio of 0.2, with the Concrete Damage Plasticity model being utilized. The concrete damage plasticity model has been widely used by many researchers (Kmiecik & and Kamiński, 2015; Deng et al., 2022), as it effectively captures the non-linear mechanical behavior of concrete. Specifically, by defining damage parameters (DAMAGEC and DAMAGET) in the model, the strain generated during the cracking process of the material is converted into equivalent plastic strain. This enables a quantifiable description of the damage evolution process. Previous studies (Deng et al., 2022; Lee et al., 2020) have demonstrated that the tensile damage parameter (DAMAGET) defined in Abaqus serves as an effective indicator for characterizing and quantifying the degree of concrete damage. This study aims to explore the fracture and failure evolution of pipe segments during jacking under deflection conditions, specifically when excessive jacking force leads to failure. Since this failure mode primarily manifests as concrete compression failure, only the compressive damage parameter (DAMAGEC) of concrete is used in the numerical model to characterize the material behavior. The relationship between compressive stress and inelastic strain in concrete is shown in Fig. 15 (supplementary data).

The rebar and steel casing are represented by an elastic constitutive model, having an elastic modulus of 200 GPa, a density of 7,850 kg/m³, and a Poisson's ratio of 0.3. Since the wooden spacer is not the primary focus of this study, its elastic modulus is set to a fixed value of 1 GPa, with a density of 600 kg/m³ and a Poisson's ratio of 0.25.

Model Development

(1) Deflection Model and Boundary Conditions

In this simulation, the deflection contact point is set at the top of the pipe joint. To accurately simulate the deflection state of the field pipe joints, the displacement and rotation of the spigot end of Pipe #1 are fully constrained, simulating a rigid connection with the already installed pipe segment. The vertical and horizontal displacements of the spigot end of Pipe #2 are restricted to eliminate the interference of gravitational settlement on the deflection analysis. The controlled relative deflection between Pipe #1 and Pipe #2 is achieved by applying an upward rotational angle at the bell end of Pipe #2. Additionally, a pressure is exerted on the wooden spacer of Pipe #2 to replicate the jacking process while the pipe segment is in a deflected state. The specific configuration is shown in Fig. 16 (supplementary data).

(2) Analysis Steps

a. A small jacking force is applied at the wooden spacer assembled at the bell end of Pipe #2 to simulate the linear jacking process of the pipe segment in a non-deflected state.
b. An upward rotational angle is applied to the surface of the bell end of Pipe #2. By parameterizing and inputting different angle values, the relative rotational angle between Pipe #1 and Pipe #2 is precisely controlled.
c. The jacking force applied at the wooden spacer on the bell end of Pipe #2 is gradually increased, enabling the simulation of different jacking forces for the pipe segment under the same deflection angle.
d. Subsequently, adjustments are made to both the upward rotational angle of the bell end surface of Pipe #2 and the applied jacking force on the wooden spacer to simulate the pipe segment under varying jacking forces and deflection angles.

(3) Meshing

During the meshing process, the mesh density near the pipe joint, as well as at the wooden spacer and steel casing, is refined, as shown in Fig. 17 (supplementary data). After meshing, the pipe segment is divided into 6,264 elements with 8,640 nodes; the wooden spacer is divided into 336 elements with 896 nodes; and the steel casing is divided into 1,064 elements with 2,432 nodes.

ANALYSIS OF RESULTS

By gradually increasing the jacking force at different deflection angles, the ultimate jacking forces for the pipe segment at deflection angles of 0.25°, 0.5°, 0.75°, and 1° were found to be 980t, 650t, 430t, and 150t, respectively. Based on these results, a curve showing the variation of the ultimate jacking force with respect to the pipe segment deflection angle was plotted, as shown in Fig. 18 (supplementary data).

As seen in Fig.18, the ultimate jacking force of the concrete pipe segment progressively diminishes as the deflection angle increases. The ultimate jacking force decreased by 33.7% as the deflection angle rose from 0.25° to 0.5°, and by 49.7% when the angle rose from 0.5° to 0.75°. This indicates that when the deflection angle exceeds 0.5°, the rate of decrease in the ultimate jacking force sharply increases: for every 0.1° increase in deflection angle, the ultimate jacking force decreases by an average of approximately 19.8%. This behavior can be attributed to the fact that at smaller deflection angles, the surface area in contact between the pipe segments remains relatively large, allowing for effective transmission of the jacking force. However, when the deflection angle exceeds 0.5°, the surface area in contact between the pipe segments significantly reduces. With the increase in deflection angle, the contact area progressively shrinks toward the edges, causing stress to concentrate excessively. The local compressive stress could easily surpass the concrete's ultimate compressive strength, which would considerably reduce the total load-bearing capacity of the pipe segment. Therefore, the rate of decrease in the ultimate jacking force is more gradual at smaller deflection angles compared to larger deflection angles.

Taking a deflection angle of 1° as an example, the stress distribution at the concrete failure point of the joint of Pipe #2 is shown in Fig. 19. Fig. 19 (a) (supplementary data). clearly demonstrates that, under the jacking condition with deflected pipe segments, the axial stress is unevenly distributed along the axis, exhibiting a gradient trend from the end to the center, gradually decreasing. Significant stress concentration is observed at the deflection point, with the local axial stress reaching 52.53 MPa, exceeding the ultimate compressive strength of C50 concrete. This indicates that concrete in this region has undergone crushing failure. As the jacking force continues to increase, stress softening occurs at the pipe joint, with the maximum axial stress decreasing from 52.53 MPa to 31.82 MPa, as shown in Fig. 19 (b) (supplementary data). At the same time, the peak compressive stress extends circumferentially on both sides of the pipe joint, while the axial stress concentration area at the deflection point increases in size. This suggests that after concrete failure, the axial stress undergoes redistribution, and the load borne by the concrete is transferred to the pipe joint and pipe barrel structures adjacent to the damaged area.

Fig. 20 (supplementary data) illustrates the distribution of concrete compressive damage in Pipe #2 at the ultimate jacking state for various deflection angles. As represented in the figure, under the deflected condition, the concrete compressive damage factor at the pipe joint for all conditions reaches 0.9334, indicating that the concrete has lost its load-bearing capacity. The damage distribution in the concrete failure region exhibits an "arch" shape, and with the increase in deflection angle, the area where the concrete loses its load-bearing capacity becomes more concentrated, extending along the axis of the pipe segment towards the pipe barrel. Notably, when the pipe segment deflects by 0.25°, in addition to the concrete failure at the joint, the concrete in the pipe barrel also experiences varying degrees of damage, manifesting as two irregular diagonal cracks. This suggests that at smaller deflection angles, the concrete in the pipe barrel develops cracks before the concrete at the pipe joint completely loses its load-bearing capacity.

To investigate the development of concrete compressive damage in the Pipe #2 beyond the limit jacking force, the subsequent damage factor trends of the pipe segment at deflections of 0.25°, 0.5°, 0.75°, and 1° after concrete failure at the pipe joint are shown in Fig. 21 (supplementary data). As seen in Fig 21, with the enhancement of the jacking force, at a deflection of 0.25°, the damaged area at the pipe joint expands, with the number of diagonal cracks increasing from 2 to 4, and the width of the initial two cracks also increases. At a deflection of 0.5°, as the jacking force continues to increase, in addition to the expansion of the damaged area at the pipe joint, diagonal cracks begin to develop from the pipe joint damage region into the pipe barrel. At deflection angles of 0.75° and 1°, further increasing the jacking force results in the damage mainly concentrated at the pipe joint, where the concrete undergoes significant failure and radiates towards the pipe barrel. The damage region evolves from an "arch" shape to a "trapezoidal" shape. Furthermore, the damage to the pipe barrel is primarily characterized by axial, near-through cracks, with no significant development of diagonal cracks observed.

Analysis of the stress distribution reveals that, at joint deflection angles of 0.25° and 0.5°, the shear stress distribution along the pipe barrel closely aligns with the observed propagation pattern of diagonal cracks, indicating that these cracks are primarily induced by shear action. The shear stress distributions are shown in Fig.22. Fig.22 (a) (supplementary data) corresponds to the 0.25° deflection case, where the first diagonal crack has just initiated in the pipe barrel while the pipe joint structure remains intact; Fig.22 (b) (supplementary data)illustrates the shear stress distribution under the deformation state depicted in Fig.21 (b).

In summary, excessive jacking force leads to pipe segment damage that is influenced by the deflection angle. At smaller deflection angles, in addition to the loss of load-bearing capacity at the pipe joint, diagonal cracks also appear in the pipe barrel. At larger deflection angles, the primary damage manifests as extensive crushing failure of the concrete at the pipe joint, with the damage radiating outward toward the pipe barrel. The cracks predominantly take a straight-line shape. Therefore, it can be concluded that in this project, with relatively small deflection angles, microcracks initially form at the pipe joint under a large jacking force.

CONCLUSION

This study, through on-site experiments of reinforced concrete jacking pipes in rock strata and numerical simulations of concrete damage development in pipe segments under deflection conditions, leads to the following conclusions:

(1) When the pipe is normally jacked through the rock strata, the contact pressure on the pipe segment is mainly distributed as follows: bottom > left side ≈ right side > top. The mud pressure is mainly distributed as top > left side ≈ right side > bottom. The contact pressure and mud pressure trends on both the left and right sides follow a similar pattern, suggesting that the mud pressure predominantly governs the surrounding contact pressure.

(2) When the pipe segment is jacked with a small deflection angle toward the upper right, significant fluctuations occur in the right-side contact pressure, left-bottom steel bar stress, and concrete strain. This phenomenon arises, because the deflection of the pipe segment causes abnormal increases in the right-side contact pressure, left-bottom steel bar stress, and concrete strain. Although the jacking machine's alignment correction temporarily restores the stress state, further deflections during the jacking process trigger another round of alignment correction. This cyclic process causes the monitoring data to fluctuate sharply.

(3) As the deflection angle increases, the ultimate jacking force of the concrete pipe segment gradually decreases. After the deflection angle exceeds 0.5°, the rate of decrease in the ultimate jacking force increases significantly.

(4) The damage pattern of the pipe segment is influenced by the deflection angle when the jacking force exceeds the limit: at smaller deflection angles, in addition to the failure of the joint concrete, diagonal cracks also appear in the pipe barrel. At larger deflection angles, the damage primarily manifests as extensive crushing of the joint concrete, with damage radiating outward and the cracks mainly taking a straight-line form.

(5) This study employs the Concrete Damaged Plasticity (CDP) model, which has certain limitations: the DAMAGEC output from the CDP model cannot be directly equated to visible macroscopic cracking or crushing. Therefore, future work should focus on developing user-defined subroutines or plugins capable of explicitly simulating the initiation and evolution of concrete cracking and crushing, thereby enabling a more intuitive and accurate investigation of damage progression in pipe segments under angular deflection.

REFERENCES

Bergeson, W. (2014). Review of long drive microtunneling technology for use on large scale projects. *Tunnelling and Underground Space Technology, 39*, 66-72. https://doi.org/10.1016/j.tust.2013.02.001

Deng, Z., Liu, X., Chen, P., De La Fuente, A., Zhao, Y., Liang, N., Zhou, X., Du, L., & Han, Y. (2022). Basalt-polypropylene fiber reinforced concrete for durable and sustainable pipe production. Part 2: Numerical and parametric analysis. *Structural Concrete, 23*(1), 328-345. https://doi.org/10.1002/suco.202000760

Hasani, S.M.R. (2025). Numerical investigation on load-bearing capacity of K-joint concrete-filled steel tube under static loading. *Jordan Journal of Civil Engineering, 19*(2). https://doi.org/10.14525/JJCE.v19i2.05

He, Y., Cheng, J., Shi, Z., Zhang, B., Chen, L., Li, X., Wang, X., & Zhang, P. (2024). Research on axial stress and strain characteristics of reinforced-concrete curved pipe jacking in power tunnels. *Buildings, 14*(9), Article 3030. https://doi.org/10.3390/buildings14093030

Kmiecik, P., & Kamiński, M. (2011). Modeling of reinforced concrete structures and composite structures with concrete strength degradation taken into consideration. *Archives of Civil and Mechanical Engineering, 11*(3), 623-636. https://doi.org/10.1016/S1644-9665(12)60105-8

Labibzadeh, M. (2015). The numerical simulations of the strengthened RC slabs with CFRPs using standard CDP material model of ABAQUS code. *European Journal of Environmental and Civil Engineering, 19*(10), 1268-

1287. https://doi.org/10.1080/19648189.2015.1013637

Lee, S.-H., Abolmaali, A., Shin, K.-J., & Lee, H.-D. (2020). ABAQUS modeling for post-tensioned reinforced concrete beams. *Journal of Building Engineering, 30*, Article 101273. https://doi.org/10.1016/j.jobe.2020.101273

Li, Y. (2020). *Study on mechanical properties of concrete pipe joint with large section in long distance pipe jacking engineering* (Doctoral dissertation, Chongqing University). https://doi.org/10.27670/d.cnki.gcqdu.2020.003703

Liu, K., Chen, X., Zhang, P., Ma, B., Feng, X., Zhang, Y., Liu, H., Tan, X., & Xu, T. (2024). Axial mechanical response of concrete pipe jacking considering the deflection of the bell-and-spigot joint: Full-scale test and numerical simulation. *Tunnelling and Underground Space Technology, 149*, Article 105805. https://doi.org/10.1016/j.tust.2024.105805

Liu, K., Xiao, A., Zhang, P., Zhou, H., Chen, Z., Xu, T., Ma, B., Ai, H., & Wang, Q. (2022). Study on mechanical response of steel pipe jacking considering the effect of pipe sticking. *Tunnelling and Underground Space Technology, 127*, Article 104617. https://doi.org/10.1016/j.tust.2022.104617

Ma, B.S. (2008). *Trenchless engineering*. People's Transportation Press.

Ma, B., & Najafi, M. (2008). Development and applications of trenchless technology in China. *Tunnelling and Underground Space Technology, 23*(4), 476-480. https://doi.org/10.1016/j.tust.2007.08.003

Milligan, G. W. E., & Norris, P. (1996). Site-based research in pipe jacking—Objectives, procedures and a case history. *Tunnelling and Underground Space Technology, 11*, 3-24. https://doi.org/10.1016/0886-7798(95)00041-0

Milligan, G.W.E., & Norris, P. (1999). Pipe-soil interaction during pipe jacking. *Proceedings of the Institution of Civil Engineers: Geotechnical Engineering, 137*(1), 27-44. https://doi.org/10.1680/gt. 1999.370104

Tong, K.M., Yang, C.S., Gao, Z.Y., & Huang, X.Y. (2020). Mechanical response and influencing factors on pipe jacking under eccentric load. *Chinese Journal of Underground Space and Engineering, 16*(5), 1459-1466. https://doi.org/10.20174/j.juse.2020.05.023

Wei, G., Xu, R. Q., & Yu, J.Y. (2005). Site-based experimental study on pipe behavior during pipe jacking. *Rock and Soil Mechanics, 26*(8), 1273-1278. https://doi.org/10.16285/j.rsm.2005.08.019

Xu, Y., Xu, Z., Zhang, C., Zhang, X., & Zhao, Z. (2025). Numerical simulation study on the mechanical properties of rectangular pipe jacking tunnel joints with longitudinal connectors. *Results in Engineering, 28*, Article 107874. https://doi.org/10.1016/j.rineng.2025.107874

Xu, Y., Zhao, Z., Zhang, C., & Lin, H. (2025). Study on shear mechanical response of F-type socket joint in rectangular pipe jacking with longitudinal connectors. *Structural Concrete*. Advance online publication. https://doi.org/10.1002/suco.70240

Zhang, P., Feng, X., Zeng, C., & Ariaratnam, S. T. (2022). Field performance of steel pipes during curve jacking in Gongbei Tunnel. *Tunnelling and Underground Space Technology, 128*, Article 104585. https://doi.org/10.1016/j.tust.2022.104585

Zhang, P., Zhang, Y., Ariaratnam, S. T., Ma, B., Zeng, C., & Liu, K. (2023). Field monitoring and analysis of soil deformation of curved steel pipe jacking in Gongbei Tunnel. *Tunnelling and Underground Space Technology, 138*, Article 105153. https://doi.org/10.1016/j.tust.2023.105153

Zhang, Y., Feng, X., Zhou, H., Zhang, P., Ma, B., Tan, L., & Wang, J. (2022). Pressure characteristics of rectangular box jacking considering box-soil-lubricant interaction. *Tunnelling and Underground Space Technology, 126*, Article 104569. https://doi.org/10.1016/j.tust.2022.104569

Zhang, Y., Yan, Z. G., & Zhu, H. (2017). Site-based research on mechanical behavior of new large-diameter pipes during pipe jacking. *Chinese Journal of Geotechnical Engineering, 39*(10), 1842-1850.

Zhou, F., Fu, M., Chai, G., & Zhang, Q. (2024). Experimental study on water sealing performance of shaft pipe joints considering the effect of compression amount of rubber seal. *Journal of Xuzhou Institute of Technology (Natural Sciences Edition), 39*(4), 1-5. https://doi.org/10.15873/j.cnki.jxit.000591

Zhou, H., Huang, S., Zhang, P., Ma, B., Ma, P., & Feng, X. (2023). Prediction of jacking force using PSO-BPNN and PSO-SVR algorithms in curved pipe roof. *Tunnelling and Underground Space Technology, 138*, Article 105159. https://doi.org/10.1016/j.tust.2023.105159